

Construction of N,N' -di(3-pyridyl)adipoamide-based Zn(II) and Cd(II) coordination networks by tuning the isomeric effect of polycarboxylate ligands†

Cite this: *CrystEngComm*, 2013, 15, 10346

Pei-Chi Cheng,^a Ming-Hao Wu,^a Ming-Yuan Xie,^a Wun-Jhih Huang,^a Hsiu-Yi He,^a Tsung-Tai Wu,^a Yang-Chih Lo,^a Davide M. Proserpio^{bc} and Jhy-Der Chen^{*a}

Eight new Zn(II) and Cd(II) coordination networks containing N,N' -di(3-pyridyl)adipoamide (**L**) and polycarboxylate ligands, $\{[Zn_2(2,5\text{-PDC})_2(\mathbf{L})(H_2O)_2] \cdot 2H_2O\}_\infty$ ($H_2PDC = 2,5\text{-pyridinedicarboxylic acid}$), **1**, $[Zn_2(2,6\text{-PDC})_2(\mathbf{L})]_\infty$, **2**, $\{[Zn_2(3,4\text{-PDC})_2(\mathbf{L})(H_2O)_6] \cdot 4H_2O\}_\infty$, **3**, $\{[Cd(2,6\text{-PDC})(\mathbf{L})(H_2O)] \cdot 4H_2O\}_\infty$, **4**, $[Zn(1,3,5\text{-HBTC})]_\infty$ ($H_3BTC = \text{benzenetricarboxylic acid}$), **5**, $\{[Cd(1,2,3\text{-HBTC})(\mathbf{L})(H_2O)] \cdot H_2O\}_\infty$, **6**, $\{[Cd_2(1,3,5\text{-HBTC})_2(\mathbf{L})(H_2O)_2] \cdot 2H_2O\}_\infty$, **7**, and $\{[Zn_3(1,2,4\text{-BTC})_2(\mathbf{L})(H_2O)_4] \cdot 4H_2O\}_\infty$, **8**, have been synthesized by hydrothermal reactions and characterized by single crystal X-ray crystallography. Structural analysis reveals that **1** and **2** form pleated **hcb** layers with 1D helical chains, in which the layers of **1** interdigitate with each other and those of **2** are linked by the π - π stacking interactions. Complexes **3** and **4** exhibit 1D ladders with single and double rungs, respectively, whereas **5** shows a 2D pleated net with the **sql** topology, **6** displays a 3D **dia** coordination network and **7** forms a 2D structure with the $(6^3)(6^6)\text{-}3,4L88$ topology. The BTC^{3-} ligands in **8** adopt the μ_4 -bonding modes, resulting in a 3D coordination network with the rare $(6^5\text{-}8)\text{-}hxg\text{-d-}4\text{-}P2/c$ topology. The various bonding modes, the ligand-isomerism of the polycarboxylate ligands and the identity of the metal center play important roles in determining the structural diversity. Their thermal and luminescent properties are also discussed.

Received 16th August 2013,
Accepted 7th October 2013

DOI: 10.1039/c3ce41622d

www.rsc.org/crystengcomm

Introduction

The design and synthesis of coordination architectures with controlled dimensionality is a rapidly developing field in supramolecular chemistry and crystal engineering.¹ These new complexes thus prepared have attracted a great attention not only due to their intriguing topological features but also their potential applications in areas such as gas storage, separation, catalysis, ion exchange and magnetism. Apart from using multidentate ligands as building blocks to form high-dimensional frameworks through coordinate-covalent bonding,² the hydrogen bonds³ and other weak interactions⁴ are also employed to increase the dimensionalities of the target products. A judicious choice of

spacer ligand with diverse functionalities and metal-ion template may lead to well-defined coordination networks. Moreover, the structural types are also affected by factors such as the metal-to-ligand ratio,⁵ the counterion,⁶ and the solvent.⁷ Although enormous examples of interesting coordination networks⁸ have been reported,¹ the control of structural dimensionality remains a challenge in the field of crystal engineering.

The mixed ligand assembly system has been widely adopted for the generation of new coordination networks.^{9,10} We have reported a series of coordination networks based on the isomeric N,N' -di(2-pyridyl)adipoamide, N,N' -di(3-pyridyl)adipoamide (**L**), N,N' -di(4-pyridyl)adipoamide, and benzenedicarboxylate ligands.^{10a} The structural types of these Zn(II) and Cd(II) coordination networks are subject to the changes of the donor atom positions of the spacer ligands, leading to the formation of a 1D double-looped chain, a 1D chain with loops, a 1D ladder, 2D layer with loops, 3-fold interpenetrated **hcb** layers, planar and undulated **hcb** layers and one 3D self-catenated net.^{10a} The net symbol of the sort **sql** or **hxg-d** are RCSR (Reticular Chemistry Structure Resource)¹¹ which are the three-letter-symbols proposed by Mike O'Keeffe¹² as the code-name for nets (similar to zeolites names), in order to identify unique topologies and avoid/minimize errors.

^a Department of Chemistry, Chung-Yuan Christian University, Chung-Li, Taiwan.
E-mail: jdchen@cycu.edu.tw

^b Università degli Studi di Milano, Dipartimento di Chimica, Via Golgi 19, 20133 Milano, Italy

^c Samara Center for Theoretical Materials Science (SCTMS), Samara State University, Ac. Pavlov St. 1, Samara 443011, Russia

† Electronic supplementary information (ESI) available: TGA curves for 1–8 (Fig. S1 and S2). Packing diagrams of **1** (Fig. 3), **3** (Fig. 4), **4** (Fig. 5) and **5** (Fig. 6). Emission spectra for H_3BTC ligands and 1–8 (Fig. S7). PXRD patterns for 1–8 (Fig. S8–S15). Selected bond distances (Å) and angles (°) for 1–8 (Table S1). CCDC numbers 949402–949409. For ESI and crystallographic data in CIF or other electronic format see DOI: 10.1039/c3ce41622d.

In our continuing efforts to investigate the correlation between the mixed-ligand system and the structural diversity of novel coordination networks, we sought to investigate the isomeric effect of the polycarboxylate ligands with more donor atoms, involving pyridinedicarboxylate and benzenetricarboxylate ligands, on the construction of *N,N'*-di(3-pyridyl)adipoamide-based Zn(II) and Cd(II) coordination networks. The syntheses, crystal structures and thermal and luminescent properties of $\{[Zn_2(2,5-PDC)_2(L)(H_2O)_2] \cdot 2H_2O\}_\infty$ [$H_2PDC = 2,5$ -pyridinedicarboxylic acid], **1**, $[Zn_2(2,6-PDC)_2(L)]_\infty$, **2**, $\{[Zn_2(3,4-PDC)_2(L)(H_2O)_6] \cdot 4H_2O\}_\infty$, **3**, $\{[Cd(2,6-PDC)(L)(H_2O)] \cdot 4H_2O\}_\infty$, **4**, $[Zn(1,3,5-HBTC)(L)]_\infty$ ($H_3BTC =$ benzenetricarboxylic acid), **5**, $\{[Cd(1,2,3-HBTC)(L)(H_2O)] \cdot H_2O\}_\infty$, **6**, $\{[Cd_2(1,3,5-HBTC)_2(L)(H_2O)_2] \cdot 2H_2O\}_\infty$, **7**, and $\{[Zn_3(1,2,4-BTC)_2(L)(H_2O)_4] \cdot 4H_2O\}_\infty$, **8**, form the subject of this report.

Experimental section

General procedures

Elemental analyses were obtained from a HERAEUS VaruoEL analyzer. The IR spectra (KBr disk) were recorded on a Jasco FT/IR-460 plus spectrometer. Thermal gravimetric analyses (TGA) measurements were carried on a TG/DTA 6200 analyzer of SII Nano Technology Inc. from 30 to 900 °C at a heating rate of 10 °C min⁻¹ under nitrogen. The emission spectra were obtained from a Hitachi F-4500 spectrometer.

Materials

The reagents $Zn(CH_3COO)_2 \cdot 2H_2O$, $Cd(CH_3COO)_2 \cdot 2H_2O$, 2,5- H_2PDC (2,5-pyridinedicarboxylic acid), 2,6- H_2PDC (2,6-pyridinedicarboxylic acid), 3,4- H_2PDC (3,4-pyridinedicarboxylic acid), 1,2,3- H_3BTC (1,2,3-benzenetricarboxylic acid), 1,2,4- H_3BTC (1,2,4-benzenetricarboxylic acid) and 1,3,5- H_3BTC (1,3,5-benzenetricarboxylic acid) were purchased from Aldrich Chemical Co. The ligand *N,N'*-di(3-pyridyl)adipoamide (**L**) was prepared according to published procedures.¹³

Preparations

$\{[Zn_2(2,5-PDC)_2(L)(H_2O)_2] \cdot 2H_2O\}_\infty$, **1**. A mixture containing $Zn(CH_3COO)_2 \cdot 2H_2O$ (0.044 g, 0.20 mmol), 2,5- H_2PDC (0.033 g, 0.20 mmol), **L** (0.030 g, 0.10 mmol) and H_2O (10 mL) was placed in a 23 mL Teflon lined stainless container. The container was then sealed and heated at 120 °C for 48 h under autogeneous pressure and then cooled slowly to room temperature. Colorless block crystals were collected, washed by ether and then dried under vacuum. Yield: 0.064 g (77%, based on Zn). Anal calcd for $C_{15}H_{16}N_3O_7Zn$ (Mw = 415.68): C, 43.34; H, 3.88; N, 10.11%. Found: C, 43.30; H, 3.64; N, 10.25%. IR (cm⁻¹): 3133(br), 1679(s), 1644(w), 1606(s), 1559(w), 1483(w), 1432(m), 1400(s), 1369(m), 1283(m), 766(w).

$[Zn_2(2,6-PDC)_2(L)]_\infty$, **2**. **2** was prepared as described for **1**, except that 2,6- H_2PDC (0.033 g, 0.20 mmol) was used. Yield: 0.052 g (68%, based on Zn). Anal calcd for $C_{15}H_{12}N_3O_5Zn$ (Mw = 379.65): C, 47.45; H, 3.19; N, 11.07%. Found: C, 47.25; H, 2.95; N, 10.93%. IR (cm⁻¹): 3130(br), 1708(s), 1644(m),

1619(m), 1584(m), 1554(s), 1487(m), 1438(w), 1421(w), 1398(w), 1363(m), 1285(s), 1164(w).

$\{[Zn_2(3,4-PDC)_2(L)(H_2O)_6] \cdot 4H_2O\}_\infty$, **3**. **3** was prepared as described for **1**, except that 3,4- H_2PDC (0.033 g, 0.20 mmol) was used. Yield: 0.077 g (82%, based on Zn). Anal calcd for $C_{15}H_{22}N_3O_{10}Zn$ (Mw = 469.73): C, 38.35; H, 4.72; N, 8.95%. Found: C, 38.30; H, 4.77; N, 8.59%. IR (cm⁻¹): 3127(br), 1681(s), 1623(s), 1588(s), 1549(s), 1495(w), 1478(m), 1410(s), 1325(w), 1279(m), 685(w).

$\{[Cd(2,6-PDC)(L)(H_2O)] \cdot 4H_2O\}_\infty$, **4**. **4** was prepared as described for **1**, except that $Cd(CH_3COO)_2 \cdot 2H_2O$ (0.027 g, 0.10 mmol) and 2,6- H_2PDC (0.017 g, 0.10 mmol) were used. Yield: 0.049 g (73%, based on Cd). Anal calcd for $C_{23}H_{31}CdN_5O_{11}$ (Mw = 665.93): C, 41.48; H, 4.69; N, 10.52%. Found: C, 41.57; H, 4.48; N, 10.38%. IR (cm⁻¹): 3107(br), 1691(s), 1613(s), 1586(s), 1560(s), 1484(m), 1428(m), 1372(s), 1311(w), 1278(w), 721(m), 689(w).

$[Zn(1,3,5-HBTC)(L)]_\infty$, **5**. **5** was prepared as described for **1**, except that $Zn(CH_3COO)_2 \cdot 2H_2O$ (0.022 g, 0.10 mmol) and 1,3,5- H_3BTC (0.021 g, 0.10 mmol) were used. Yield: 0.047 g (82%, based on Zn). Anal calcd for $C_{25}H_{22}N_4O_8Zn$ (Mw = 571.84): C, 52.51; H, 3.88; N, 9.80%. Found: C, 52.17; H, 3.84; N, 9.55%. IR (cm⁻¹): 3133(br), 1720(m), 1671(s), 1632(s), 1613(s), 1578(m), 1556(s), 1486(m), 1414(m), 1353(s), 1296(w), 1234(m), 1179(w), 673(w).

$\{[Cd(1,2,3-HBTC)(L)(H_2O)] \cdot H_2O\}_\infty$, **6**. **6** was prepared as described for **1**, except that $Cd(CH_3COO)_2 \cdot 2H_2O$ (0.027 g, 0.10 mmol) and 1,2,3- H_3BTC (0.021 g, 0.10 mmol) were used. Yield: 0.057 g (86%, based on Cd). Anal calcd for $C_{25}H_{26}CdN_4O_{10}$ (Mw = 654.90): C, 45.85; H, 4.00; N, 8.55%. Found: C, 45.79; H, 3.95; N, 8.45%. IR (cm⁻¹): 3102(br), 1682(s), 1612(s), 1578(w), 1550(s), 1484(s), 1462(w), 1385(s), 1358(s), 1286(m), 700(w).

$\{[Cd_2(1,3,5-HBTC)_2(L)(H_2O)_2] \cdot 2H_2O\}_\infty$, **7**. **7** was prepared as described for **1**, except that $Cd(CH_3COO)_2 \cdot 2H_2O$ (0.053 g, 0.20 mmol) and 1,3,5- H_3BTC (0.042 g, 0.20 mmol) were used. Yield: 0.098 g (97%, based on Cd). Anal calcd for $C_{17}H_{17}CdN_2O_9$ (Mw = 505.73): C, 40.37; H, 3.39; N, 5.54%. Found: C, 40.37; H, 3.34; N, 5.49%. IR (cm⁻¹): 3126(br), 1709(w), 1677(s), 1621(w), 1585(w), 1546(s), 1421(s), 1398(m), 1371(s), 1279(s), 740(m), 689(w).

$\{[Zn_3(1,2,4-BTC)_2(L)(H_2O)_4] \cdot 4H_2O\}_\infty$, **8**. **8** was prepared as described for **1**, except that $Zn(CH_3COO)_2 \cdot 2H_2O$ (0.066 g, 0.30 mmol) and 1,2,4- H_3BTC (0.042 g, 0.20 mmol) were used. Yield: 0.095 g (91%, based on Zn). Anal calcd for $C_{17}H_{20}N_2O_{11}Zn_{1.5}$ (Mw = 526.41): C, 38.79; H, 3.83; N, 5.32%. Found: C, 39.12; H, 3.80; N, 5.26%. IR (cm⁻¹): 3134(br), 1696(s), 1618(m), 1590(s), 1552(s), 1485(m), 1417(m), 1369(s), 1291(w), 1250(w).

X-ray crystallography. The diffraction data for complexes **1–3**, **5** and **8** were collected on a Bruker AXS P4 diffractometer at 22 °C while those of **4**, **6** and **7** were collected on a Bruker AXS SMART APEX II diffractometer at 22 °C, which was equipped with a graphite-monochromated MoK_α ($\lambda_\alpha = 0.71073 \text{ \AA}$) radiation. The data reduction was carried by standard methods with the use of well-established computational

procedures.¹⁴ The structure factors were obtained after Lorentz and polarization correction. An empirical absorption correction based on a series of ψ -scans was applied to the data for complexes 1–3, 5 and 8, while the empirical absorption correction based on “multi-scan” was applied to the data for complexes 4, 6 and 7. The positions of some of the heavier atoms, including the zinc or cadmium atom, were located by the direct method. The remaining atoms were found in a series of alternating difference Fourier maps and least-square refinements.¹⁵ All the hydrogen atoms for complexes 1–8 were added by using the HADD command in SHELXTL 5.10. The O(1) atom of 2, O(3), O(7), O(8) and O(11) atoms of 4, C(1)–C(3), C(8) and O(11) atoms of 7 and C(8) and O(10) atoms of 8 are disordered such that two or three orientations can be found for each disordered atom. Basic information pertaining to the crystal parameters and structure refinement is summarized in Table 1. Selected bond distances and angles are listed in Table S1.†

Results and discussion

Structure of $\{[\text{Zn}_2(2,5\text{-PDC})_2(\text{L})(\text{H}_2\text{O})_2]\cdot 2\text{H}_2\text{O}\}_\infty$, 1

Fig. 1(a) shows the coordination environment of the Zn(II) ion, which is coordinated by one pyridyl nitrogen atom of the L ligand [Zn–N = 2.128(2) Å], one pyridyl nitrogen atom, two carboxylate oxygen atoms from two 2,5-PDC²⁻ ligands [Zn–N = 2.162(2), Zn–O = 2.021(2) and 2.032(2) Å] and one oxygen atom of a water molecule [Zn–O = 2.042(2) Å], resulting in a distorted square pyramidal geometry with a τ value of 0.330.¹⁶ Fig. 1(b) shows that the Zn(II) ions are bridged by the 2,5-PDC²⁻ ligands to form helical chains down [0,1,0], which are linked by the ligands L to form a 2D pleated layer with a honeycomb hcb topology as shown in Fig. 1(c). The Zn \cdots Zn distances that are bridged by 2,5-PDC²⁻ and L are 8.20 and 17.33 Å, respectively, and the 54-membered ring involving $\{\text{Zn}_6\text{N}_{12}\text{O}_4\text{C}_{32}\}$ has an approximate ring size of $14.27 \times 25.78 \text{ \AA}^2$. Noticeably, the hcb layers interdigitate with each other by directing the pyridyl rings of the L ligands into the windows of the adjacent nets, giving the final 3D supramolecular architecture, Fig. 1(d). The hcb nets are interlinked by the cocrystallized water molecules *via* N–H \cdots O (H \cdots O = 1.97 Å, $\angle\text{N–H}\cdots\text{O} = 166^\circ$) and O–H \cdots O (H \cdots O = 1.89 Å, $\angle\text{O–H}\cdots\text{O} = 176^\circ$ and H \cdots O = 1.98 Å, $\angle\text{O–H}\cdots\text{O} = 163^\circ$) hydrogen bonds. The nets are also linked by the coordinated water molecules through O–H \cdots O (H \cdots O = 1.87 Å, $\angle\text{O–H}\cdots\text{O} = 173^\circ$ and H \cdots O = 2.02 Å, $\angle\text{O–H}\cdots\text{O} = 175^\circ$) hydrogen bonds, Fig. S3.†

Structure of $[\text{Zn}_2(2,6\text{-PDC})_2(\text{L})]_\infty$, 2

The coordination environment about the Zn(II) ion is shown in Fig. 2(a). The Zn(II) metal center is coordinated by one pyridyl nitrogen atom of the L ligand [Zn–N = 2.029(2) Å], one pyridyl nitrogen atom and three carboxylate oxygen atoms from two 2,6-PDC²⁻ ligands [Zn–N = 2.014(2), Zn–O = 1.959(2)–2.278(2) Å], resulting in a distorted square pyramidal geometry with a τ value of 0.287. Fig. 2(b) shows that the Zn(II) ions are bridged by the 2,6-PDC²⁻ ligands to form

helical chains down [0,1,0], which are also linked to each other through the pyridyl nitrogen atoms of the L ligands to form a 2D pleated layer with the honeycomb hcb topology as shown in Fig. 2(c). The Zn \cdots Zn distances that are bridged by 2,6-PDC²⁻ and L ligands are 5.05 and 18.91 Å, respectively, and the 38-membered ring involving $\{\text{Zn}_6\text{N}_8\text{O}_4\text{C}_{20}\}$ has an approximate ring size of $14.03 \times 25.04 \text{ \AA}^2$. In contrast to the 2D layers of 1 that are interdigitating, those of 2 are flatter and interlinked by the π – π (3.56 Å) interactions between the pyridyl rings of the 2,6-PDC²⁻ ligands, Fig. 2(d), presumably due to the different donor atom positions of the carboxylate ligands that result in different undulations of the 2D layers. The intramolecular hydrogen bonds between the N–H groups of the L ligands and the carboxylate oxygen atoms of the 2,6-PDC²⁻ ligands (H \cdots O = 2.09 Å, $\angle\text{N–H}\cdots\text{O} = 169^\circ$) are also seen in the structure.

Structure of $\{[\text{Zn}_2(3,4\text{-PDC})_2(\text{L})(\text{H}_2\text{O})_6]\cdot 4\text{H}_2\text{O}\}_\infty$, 3

Fig. 3(a) shows the coordination environment of the Zn(II) ion, which is coordinated by one pyridyl nitrogen atom of the L ligand [Zn–N = 2.155(2) Å], one pyridyl nitrogen atom and one carboxylate oxygen atom from two 3,4-PDC²⁻ ligands [Zn–N = 2.131(2), Zn–O = 2.066(2) Å] and three coordinated water molecules [Zn–O = 2.073(2)–2.265(2) Å] to form a distorted octahedral geometry. Fig. 3(b) shows that the Zn(II) ions are bridged by the L and 3,4-PDC²⁻ ligands to form a 1D ladder and Fig. 3(c) depicts its schematic drawing. The 44-membered ring involving $\{\text{Cd}_4\text{N}_{10}\text{O}_2\text{C}_{28}\}$ has an approximate ring size of $9.17 \times 15.78 \text{ \AA}^2$. The adjacent ladder chains, running parallel to [0,1,0], are linked by the N–H \cdots O (H \cdots O = 2.06 Å, $\angle\text{N–H}\cdots\text{O} = 161^\circ$) hydrogen bonds originating from the N–H groups of the L ligands to the carboxylate oxygen atoms of the 3,4-PDC²⁻ ligands, which are also linked by the O–H \cdots O hydrogen bonds originating from the cocrystallized (H \cdots O = 1.84–2.18 Å, $\angle\text{O–H}\cdots\text{O} = 143$ – 168°) and coordinated (H \cdots O = 1.84–2.23 Å, $\angle\text{O–H}\cdots\text{O} = 155$ – 173°) water molecules, Fig. S4.†

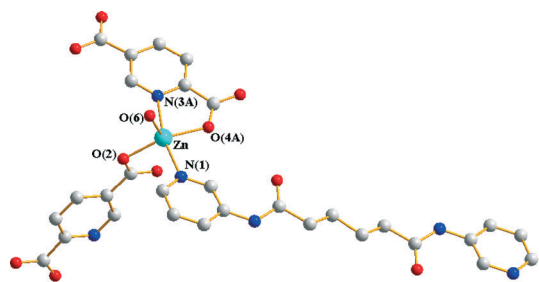
A comparison of 1–3 shows that the donor atom positions of the 2,5-, 2,6- and 3,4-PDC²⁻ ligands play an important role in determining the structures of the L-based Zn(II) coordination polymers, resulting in 2D layers with interdigitation, 2D layers linked by π – π interactions and a 1D ladder for 1–3, respectively.

Structure of $[\text{Cd}(2,6\text{-PDC})(\text{L})(\text{H}_2\text{O})]\cdot 4\text{H}_2\text{O}\}_\infty$, 4

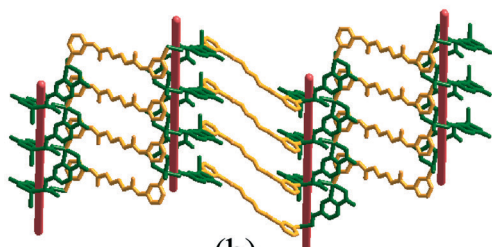
The coordination environment about the Cd(II) ion is shown in Fig. 4(a). The Cd(II) metal center is coordinated by two pyridyl nitrogen atoms of two L ligands [Cd–N = 2.353(2) and 2.367(2) Å], one pyridyl nitrogen atom and three carboxylate oxygen atoms from two 2,6-PDC²⁻ ligands [Cd–N = 2.351(2), Cd–O = 2.429(1)–2.469(2) Å] and one coordinated water molecule [Cd–O = 2.299(2) Å], resulting in a pentagonal bipyramidal geometry. One nitrogen and three oxygen atoms of two 2,6-PDC²⁻ ligands and one coordinated water molecule are located in the equatorial plane [$\angle\text{N}(5)\text{–Cd–O}(3) + \angle\text{O}(3)\text{–Cd–O}(7) + \angle\text{O}(7)\text{–Cd–O}(5\text{B}) + \angle\text{O}(5\text{B})\text{–Cd–O}(5) + \angle\text{O}(5)\text{–Cd–N}(5) = 360.38^\circ$],

Table 1 Crystal data for complexes 1–8

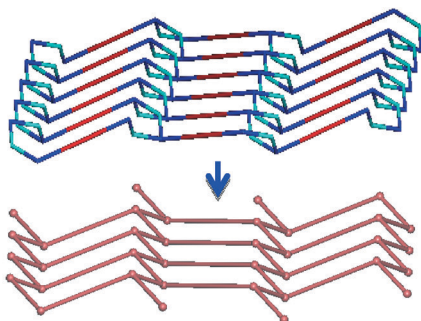
| Compound | 1 | 2 | 3 | 4 | 5 | 6 | 7 | 8 |
|--|--|--|--|--|--|--|--|--|
| Formula | C ₁₅ H ₁₆ N ₃ O ₇ Zn | C ₁₅ H ₁₂ N ₃ O ₇ Zn | C ₁₅ H ₂₂ N ₃ O ₁₀ Zn | C ₂₃ H ₃₁ CdN ₃ O ₁₁ | C ₂₃ H ₂ N ₃ O ₈ Zn | C ₂₅ H ₂₆ CdN ₄ O ₁₀ | C ₁₇ H ₁₇ CdN ₂ O ₉ | C ₁₇ H ₂₀ N ₂ O ₁₁ |
| Fw | 415.68 | 379.65 | 469.73 | 665.93 | 571.84 | 654.90 | 505.73 | Zn _{1.5} 526.41 |
| Crystal system | Monoclinic | Monoclinic | Monoclinic | Triclinic | Monoclinic | Monoclinic | Monoclinic | Monoclinic |
| Space group | <i>P2₁/n</i> | <i>P2₁/c</i> | <i>P2₁/n</i> | <i>P1</i> | <i>P2₁/n</i> | <i>P2₁</i> | <i>P2/c</i> | <i>P2₁/n</i> |
| <i>a</i> , Å | 9.7536(12) | 16.031(3) | 12.0604(13) | 10.5240(4) | 11.6305(17) | 11.3111(2) | 11.5273(1) | 6.0834(9) |
| <i>b</i> , Å | 11.3569(17) | 7.3539(8) | 9.1735(10) | 11.2622(5) | 15.905(3) | 13.8834(3) | 9.0488(1) | 20.891(2) |
| <i>c</i> , Å | 15.934(3) | 13.9631(7) | 17.818(3) | 12.3561(5) | 13.6118(15) | 16.8506(3) | 18.0697(2) | 16.210(2) |
| <i>α</i> , ° | 90 | 90 | 90 | 72.554(2) | 90 | 90 | 90 | 90 |
| <i>β</i> , ° | 107.790(11) | 109.457(7) | 100.645(12) | 74.971(2) | 95.368(14) | 99.9920(10) | 97.707(1) | 94.148(12) |
| <i>γ</i> , ° | 90 | 90 | 90 | 83.246(2) | 90 | 90 | 90 | 90 |
| <i>V</i> , Å ³ | 1680.6(5) | 1552.2(3) | 1937.4(4) | 1348.07(10) | 2506.8(6) | 2606.02(9) | 1867.79(3) | 2054.7(5) |
| <i>Z</i> | 4 | 4 | 4 | 2 | 4 | 4 | 4 | 4 |
| <i>D</i> _{calc} , g cm ⁻³ | 1.643 | 1.625 | 1.610 | 1.641 | 1.515 | 1.669 | 1.798 | 1.702 |
| <i>F</i> (000) | 852 | 772 | 972 | 680 | 1176 | 1328 | 1012 | 1076 |
| <i>μ</i> (Mo K α), mm ⁻¹ | 1.506 | 1.614 | 1.328 | 0.878 | 1.037 | 0.904 | 1.225 | 1.829 |
| Range (2 θ) for data collection, deg | 4.38 ≤ 2 θ ≤ 50.00 | 5.38 ≤ 2 θ ≤ 50.00 | 3.78 ≤ 2 θ ≤ 50.00 | 3.56 ≤ 2 θ ≤ 56.66 | 3.94 ≤ 2 θ ≤ 50.00 | 3.66 ≤ 2 θ ≤ 56.62 | 3.56 ≤ 2 θ ≤ 56.74 | 3.90 ≤ 2 θ ≤ 50.00 |
| Independent reflections | 2937 | 2721 | 3393 | 6656 | 4369 | 11 215 | 4663 | 3594 |
| Data/restraints/parameters | [<i>R</i> _(int) = 0.0268] 2937/0/251 | [<i>R</i> _(int) = 0.0274] 2721/0/226 | [<i>R</i> _(int) = 0.0274] 3393/0/302 | [<i>R</i> _(int) = 0.0184] 6656/0/397 | [<i>R</i> _(int) = 0.0224] 4369/0/343 | [<i>R</i> _(int) = 0.0785] 11 215/1/721 | [<i>R</i> _(int) = 0.0223] 4663/0/316 | [<i>R</i> _(int) = 0.0521] 3594/0/304 |
| Quality-of-fit indicator ^c | 1.058 | 1.063 | 1.039 | 1.029 | 1.049 | 0.993 | 1.048 | 1.041 |
| Final <i>R</i> indices | <i>R</i> ₁ = 0.0338, <i>wR</i> ₂ = 0.0747 | <i>R</i> ₁ = 0.0273, <i>wR</i> ₂ = 0.0685 | <i>R</i> ₁ = 0.0338, <i>wR</i> ₂ = 0.0833 | <i>R</i> ₁ = 0.0238, <i>wR</i> ₂ = 0.0624 | <i>R</i> ₁ = 0.0312, <i>wR</i> ₂ = 0.0684 | <i>R</i> ₁ = 0.0579, <i>wR</i> ₂ = 0.0658 | <i>R</i> ₁ = 0.0253, <i>wR</i> ₂ = 0.0602 | <i>R</i> ₁ = 0.0421, <i>wR</i> ₂ = 0.0950 |
| [<i>I</i> > 2 σ (<i>I</i>)] ^b | <i>R</i> ₁ = 0.0446, <i>wR</i> ₂ = 0.0800 | <i>R</i> ₁ = 0.0344, <i>wR</i> ₂ = 0.0727 | <i>R</i> ₁ = 0.0436, <i>wR</i> ₂ = 0.0885 | <i>R</i> ₁ = 0.0277, <i>wR</i> ₂ = 0.0652 | <i>R</i> ₁ = 0.0451, <i>wR</i> ₂ = 0.0739 | <i>R</i> ₁ = 0.1255, <i>wR</i> ₂ = 0.0806 | <i>R</i> ₁ = 0.0326, <i>wR</i> ₂ = 0.0634 | <i>R</i> ₁ = 0.0718, <i>wR</i> ₂ = 0.1077 |
| <i>R</i> indices (all data) | | | | | | | | |
| ^a <i>R</i> ₁ = $\Sigma F_o - F_c / \Sigma F_o $, ^b <i>wR</i> ₂ = $\Sigma w(F_o^2 - F_c^2) / \Sigma w(F_o^2)$, ^c Quality-of-fit = $[\Sigma w(F_o - F_c)^2 / N_{\text{parameters}}]^{1/2}$. | | | | | | | | |



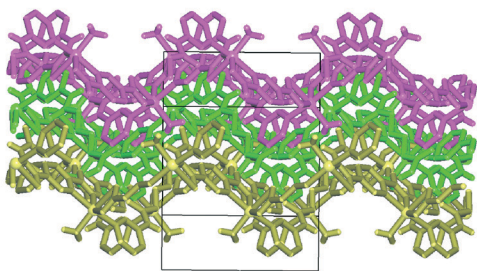
(a)



(b)

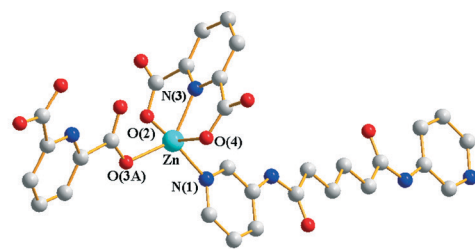


(c)

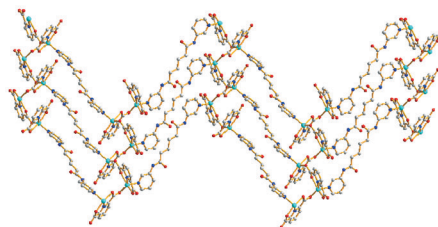


(d)

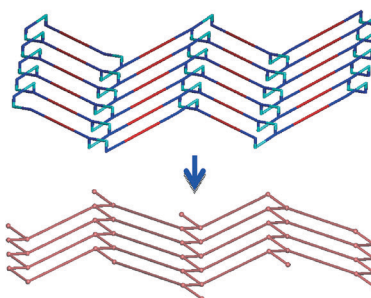
Fig. 1 (a) A drawing showing the coordination environment of the Zn(II) ion of **1**. (b) The **hcb** pleated net with helical chains. (c) A schematic drawing of the **hcb** net. (d) A view down $[-3,0,1]$, showing the interdigitation of the layers.



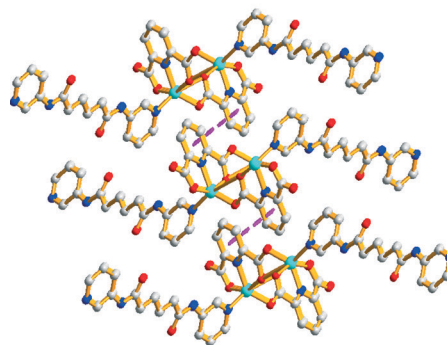
(a)



(b)



(c)



(d)

Fig. 2 (a) A drawing showing the coordination environment of the Zn(II) ion of **2**. (b) The **hcb** pleated net with helical chains. (c) A schematic drawing of the **hcb** net. (d) The 2D nets are linked by π - π interactions.

with the Cd(II) center deviating from the plane by 0.13 Å, while two pyridyl nitrogen atoms of the L ligands occupy the axial positions. Fig. 4(b) shows that the Cd(II) atoms are chelated and bridged by the 2,6-PDC²⁻ ligands to form dinuclear units, which are also linked by the L ligands to form a ladder with double bridged rungs, and Fig. 4(c) depicts

a schematic drawing. The Cd...Cd distances that are bridged by the 2,6-PDC²⁻ and L ligands are 3.40 and 19.45 Å, respectively. All the ladders run parallel to $[1,-1,-1]$. The adjacent ladders are linked by N-H...O (H...O = 1.95 Å, \angle N-H...O = 173°) hydrogen bonds between the amine groups of the L ligands and the carboxylate oxygen of the 2,6-PDC²⁻

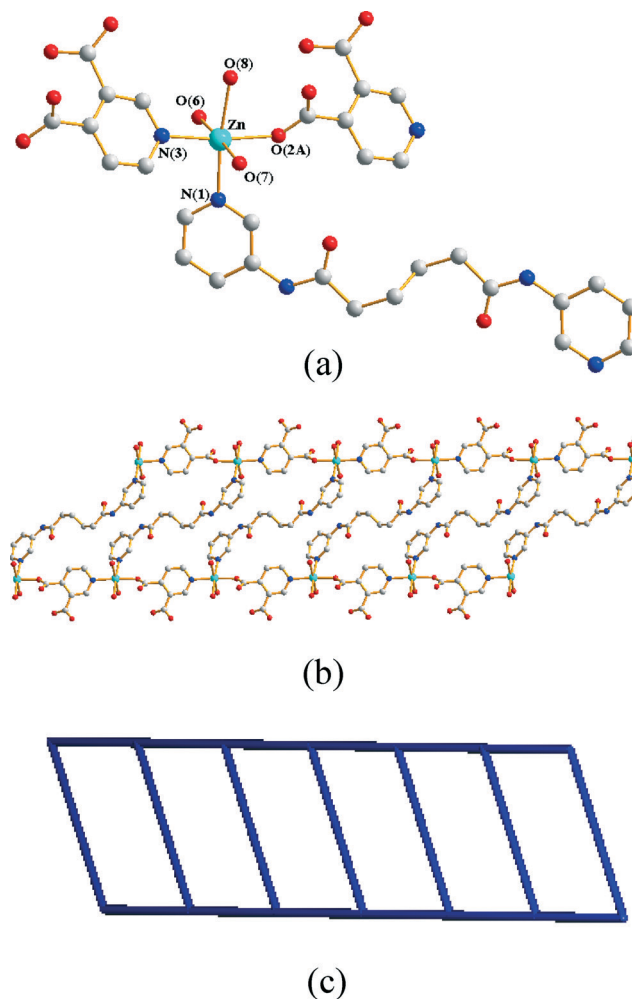


Fig. 3 (a) A drawing showing the coordination environment of the Zn(II) ion of **3**. (b) The 1D ladder with the underlying motif in (c).

ligands resulting in a single 3D supramolecular architecture, Fig. S5.†

A structural comparison of **2** and **4** reveals that the identity of the metal center is important in determining the structural diversity, presumably due to the different sizes of the Zn(II) and Cd(II) centers that result in a distorted octahedral geometry and a pentagonal bipyramidal geometry for **2** and **4**, respectively.

Structure of $[\text{Zn}(1,3,5\text{-HBTC})(\text{L})]_{\infty}$, **5**

Fig. 5(a) shows the coordination environment of the Zn(II) ion. The Zn(II) metal center is coordinated by two pyridyl nitrogen atoms of two L ligands [$\text{Zn-N} = 2.034(2)$ and $2.061(2)$ Å] and two carboxylate oxygen atoms of two 1,3,5-HBTC²⁻ ligands [$\text{Zn-O} = 1.918(2)$ and $1.935(2)$ Å], resulting in a distorted tetrahedral geometry. Fig. 5(b) shows that the Zn(II) atoms are bridged by L ligands and 1,3,5-HBTC²⁻ ligands to form a 2D pleated net and the Zn \cdots Zn distances that are bridged by the 1,3,5-HBTC²⁻ and L ligands are 9.41 and 18.53 Å, respectively. Fig. 5(c) shows a schematic drawing of the highly undulated 2D net with the square layer **sql** topology. The 2D nets are interlinked by the π - π (3.61 Å) interactions and the N-H \cdots O

hydrogen bonds between the L ligands ($\text{H}\cdots\text{O} = 2.05$, $\angle\text{N-H}\cdots\text{O} = 174^\circ$) and between the L ligand and the carboxylate oxygen of the 1,3,5-HBTC²⁻ ligand ($\text{H}\cdots\text{O} = 1.94$ Å, $\angle\text{N-H}\cdots\text{O} = 169^\circ$), Fig. S6.

Structure of $\{[\text{Cd}(1,2,3\text{-HBTC})(\text{L})(\text{H}_2\text{O})]\cdot\text{H}_2\text{O}\}_{\infty}$, **6**

Fig. 6(a) shows the asymmetric unit with two independent Cd(II) ions. Each of the Cd(II) ions are coordinated by two pyridyl nitrogen atoms of two L ligands [$\text{Cd-N} = 2.363(6)$ and $2.410(6)$ Å for Cd(1) and $2.350(6)$ and $2.470(6)$ Å for Cd(2)], three carboxylate oxygen atoms of two 1,2,3-HBTC²⁻ ligands [$\text{Cd-O} = 2.215(6)$ – $2.619(6)$ Å for Cd(1) and $2.258(5)$ – $2.591(5)$ Å for Cd(2)] and one coordinated water molecule [$\text{Cd-O} = 2.299(5)$ Å for Cd(1) and $2.310(5)$ Å for Cd(2)], resulting in the distorted octahedral geometry, Fig. 6(b) and (c). Each Cd(II) ion is connected to four neighboring Cd(II) ions through four distances that are 5.82 and 6.06 Å (through 1,2,3-HBTC²⁻) and 17.82 and 18.86 Å (through L) and thus each Cd(II) ion can be considered as a four-connected node. Topological analysis reveals that complex **6** forms a single 3D coordination network with the most common 4-connected **dia** topology, Fig. 6(d), as determined using TOPOS.¹⁷

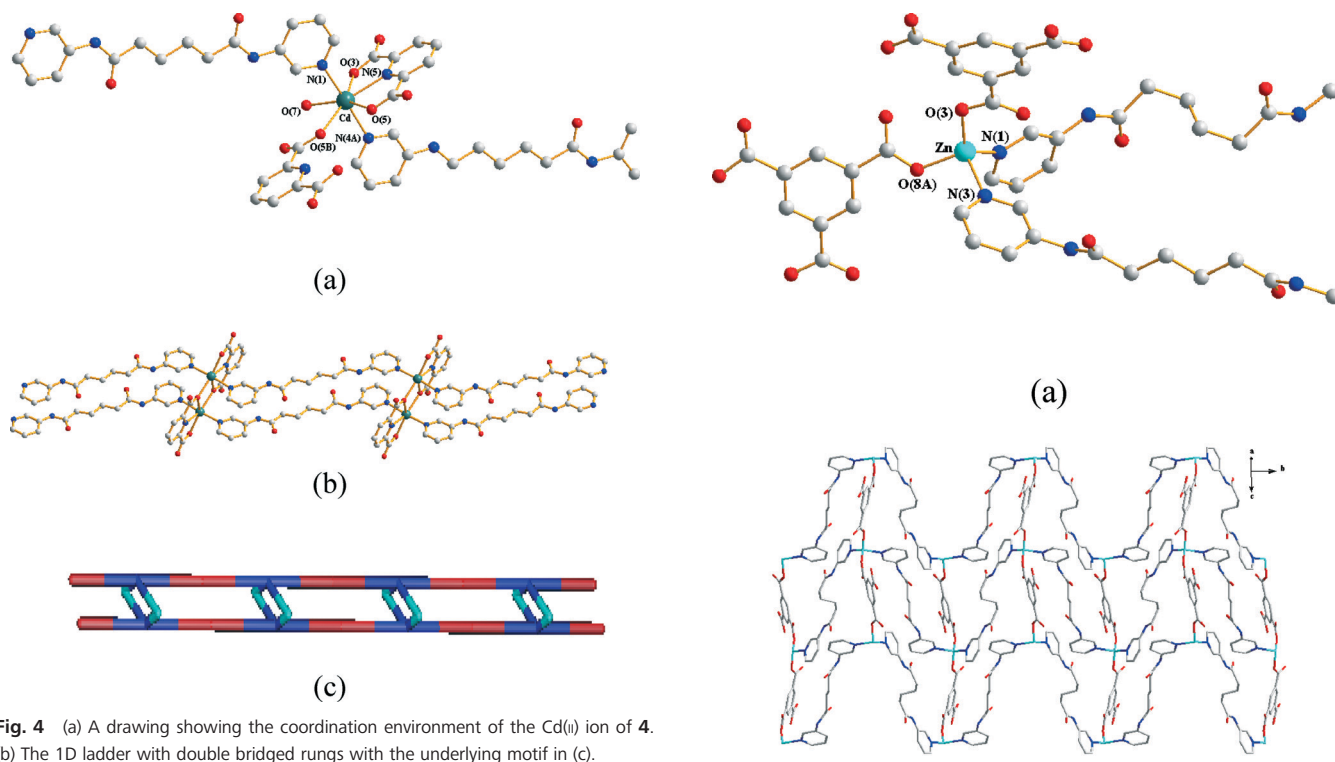


Fig. 4 (a) A drawing showing the coordination environment of the Cd(II) ion of **4**. (b) The 1D ladder with double bridged rungs with the underlying motif in (c).

Structure of $\{[\text{Cd}_2(1,3,5\text{-HBTC})_2(\text{L})(\text{H}_2\text{O})_2] \cdot 2\text{H}_2\text{O}\}_\infty$, **7**

Fig. 7(a) shows the coordination environment of the Cd(II) ion, which is coordinated by one pyridyl nitrogen atom of the L ligand [Cd–N = 2.337(2) Å], five carboxyl oxygen atoms of three 1,3,5-HBTC²⁻ ligands [Cd–O = 2.298(1)–2.510(1) Å] and one coordinated water molecule [Cd–O = 2.290(2) Å], resulting in a distorted pentagonal bipyramidal geometry. Five oxygen atoms of three 1,3,5-HBTC²⁻ ligands are located in the equatorial plane [$\angle\text{O}(3)\text{-Cd-O}(2) + \angle\text{O}(2)\text{-Cd-O}(6\text{A}) + \angle\text{O}(6\text{A})\text{-Cd-O}(7\text{A}) + \angle\text{O}(7\text{A})\text{-Cd-O}(5\text{B}) + \angle\text{O}(5\text{B})\text{-Cd-O}(3) = 359.87^\circ$] with the Cd(II) center deviating from the plane by 0.12 Å, while one pyridyl nitrogen atom of the L ligand and one water molecule occupy the axial positions. Each 1,3,5-HBTC²⁻ bridges three Cd(II) ions with distances that are 5.63, 5.64 and 5.94 Å from the center of the 1,3,5-HBTC²⁻ ligand to the Cd(II) ions, forming a three-connected node, whereas each Cd(II) ion is connected to three 1,3,5-HBTC²⁻ ligands and one Cd(II) ion (Cd...Cd = 15.51 Å, through L) and can be considered as a four-connected node. The layers stack along [1,0,0] as AAAA. Topological analysis using TOPOS reveals that complex **7** forms a binodal 3,4-connected 2D double layer with (6³)(6⁶)-3,4L88 topology, Fig. 7(b), in which hexagonal planes are pillared by the L ligands. This double layer net is rare as shown in a recent survey of the topology of more than 10 000 2-periodic coordination networks.¹⁸ Short π - π (3.53 Å) contacts between the 1,3,5-HBTC²⁻ ligands are also observed.

Structure of $\{[\text{Zn}_3(1,2,4\text{-BTC})_2(\text{L})(\text{H}_2\text{O})_4] \cdot 4\text{H}_2\text{O}\}_\infty$, **8**

Fig. 8(a) shows the coordination environment of the Zn(II) ions. There are two independent Zn(II) ions in the structure

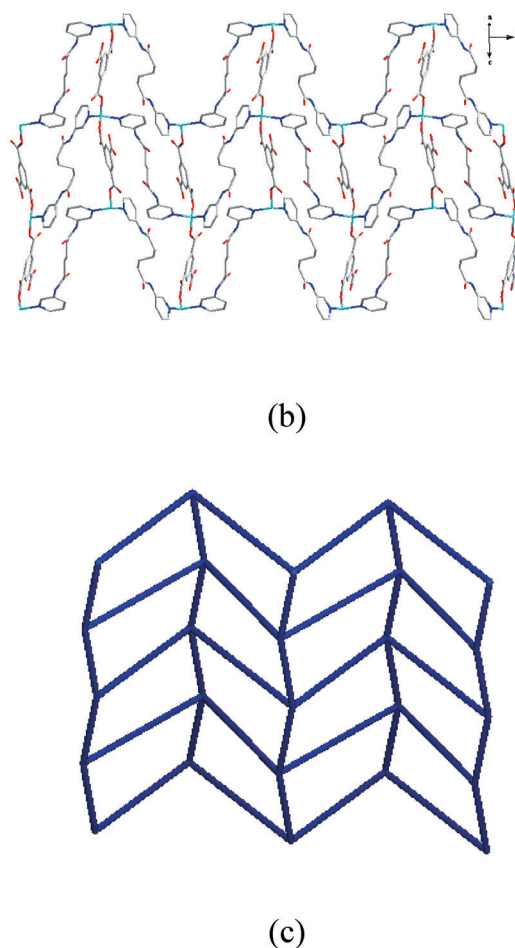


Fig. 5 (a) A drawing showing the coordination environment of the Zn(II) ion of **5**. (b) The 2D undulated net with its underlying sqI in (c).

which adopt different geometries. While the Zn(1) metal center is coordinated by one pyridyl nitrogen atom of the L ligand [Zn–N = 2.053(3) Å] and four carboxyl oxygen atoms of three 1,2,4-BTC³⁻ ligands [Zn–O = 1.963(2)–2.252(3) Å] to form a distorted square pyramidal geometry with a τ value of 0.469, the Zn(2) metal center is coordinated by two carboxylate oxygen atoms of two 1,2,4-BTC³⁻ ligands [Zn–O = 2.090(2) Å] and four coordinated water molecules [Zn–O = 2.063(4)–2.150(3) Å] to form a distorted octahedral geometry. Topologically, both the Zn(1) atom and the 1,2,4-BTC³⁻ ligand can be regarded as

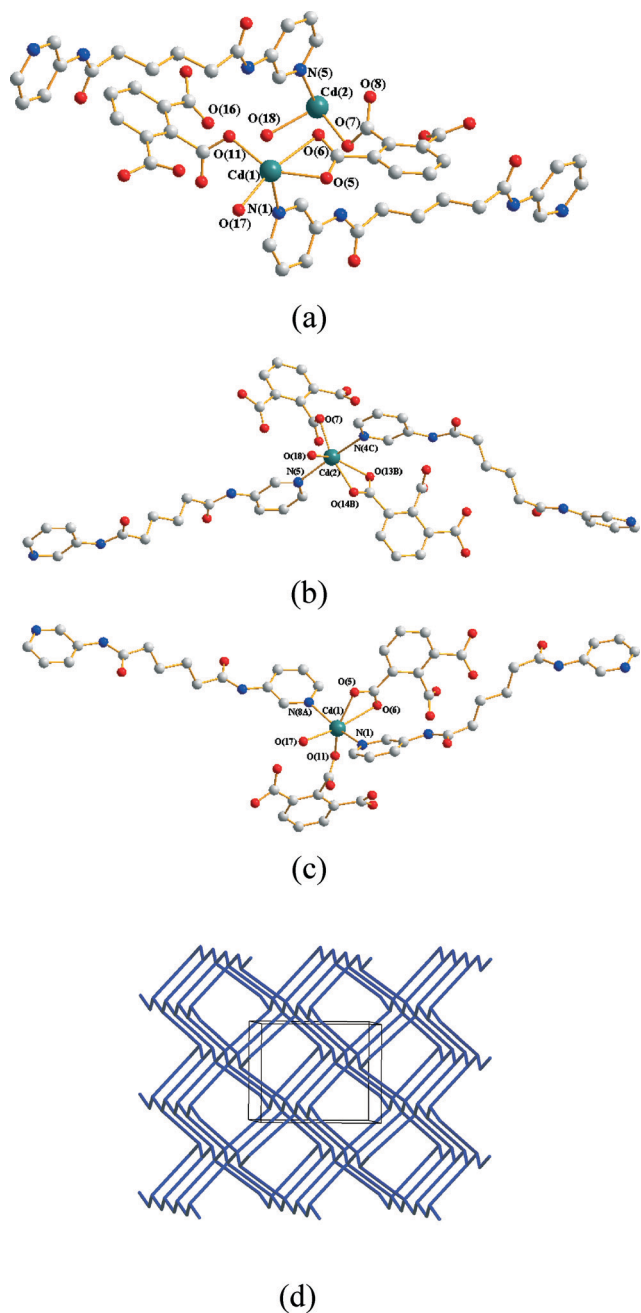


Fig. 6 (a) A drawing showing the asymmetric unit of **6**. (b) The coordination environment about the Cd(1) center and (c) the Cd(2) center. (d) A drawing showing the 3D framework with the **dia** topology.

4-connected nodes while the two-connected Zn(2) atom and L can be simplified as linkers. Each 1,2,4-HBTC²⁻ bridges three Zn(II) ions with distances that are 3.77, 4.87 and 5.82 Å from the center of the 1,2,4-HBTC²⁻ ligand to the Zn(II) ions and connect the other 1,2,4-HBTC²⁻ ligand, through Zn(1) atom, with a distance of 11.04 Å, whereas the Zn(1) nodes are also separated by L through a distance of 17.70 Å. The TOPOS program shows that the two chemically distinct nodes are topologically equivalent with the same point symbol of (6⁵·8), giving a uninodal 4-connected 3D coordination network with the (6⁵·8)-**hxg-d-4-P2/c** topology, Fig. 8(b). This is a rare net

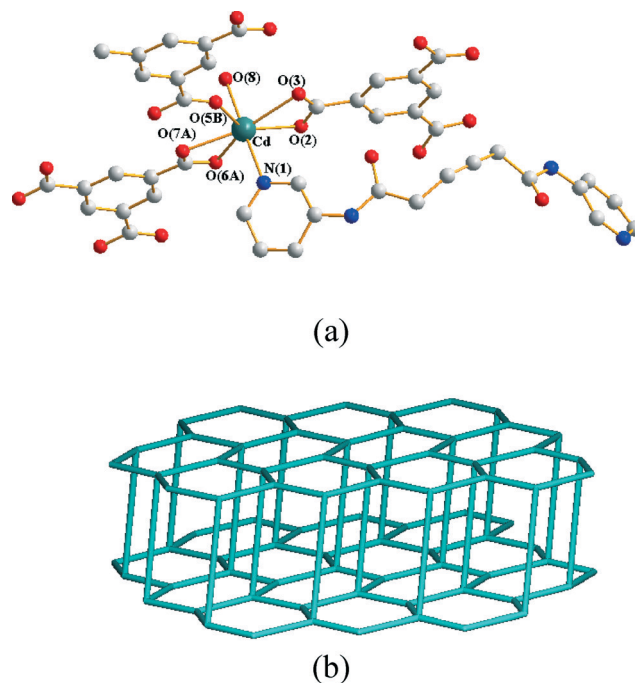


Fig. 7 (a) A drawing showing the coordination environment of the Cd(II) ion of **7**. (b) A drawing showing the 2D double layer with the 3,4L88 topology.

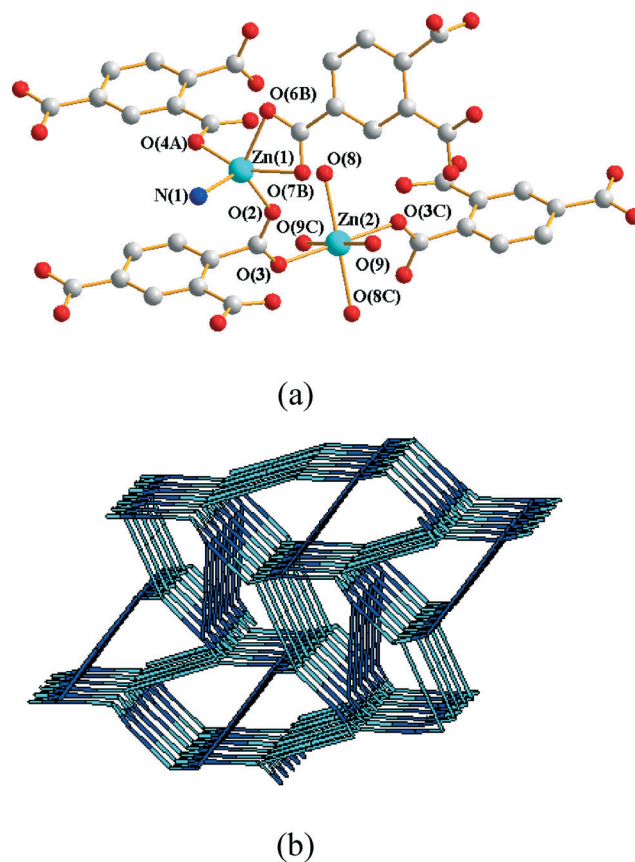


Fig. 8 (a) A drawing showing the coordination environment of the Zn(II) ions of **8**. The L ligand is represented by the N(1) atom. (b) The 3D framework with the 4-c (6⁵·8)-**hxg-d-4-P2/c** topology. Removing the long edge corresponding to the L ligand (the blue line) we get the (3,4)-**c ins** net.

derived from the 10-connected **h_xg-d** net after removing some edges according to the approach described by Blatov.¹⁹

Complex 8 represents the second example of the (6⁵-8)-**h_xg-d-4-P2/c** topology, the first one being reported in the TTO database²⁰ of TOPOS for the compound [Co₃(3-pbcd)(1,2,4-BTC)₂(H₂O)₄]-4H₂O [3-pbcd = *N,N'*-bis(pyridine-3-yl)cyclohexane-1,4-dicarboxamide)]. The two compounds are very similar also in the crystallographic parameters, but without knowing the underlying net we probably will have missed this isorecticular compound, that was described incorrectly in the original manuscript.²¹ If the long **L** ligand is disregarded, we get the more common (3,4)-c net **ins**.

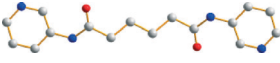
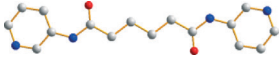
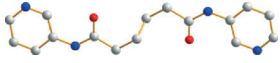
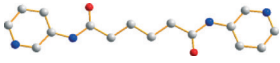
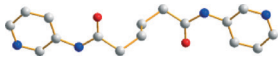
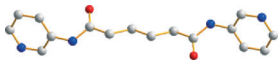
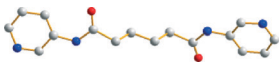
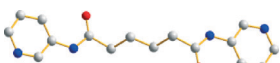
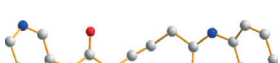
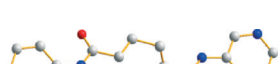
Conformations and bonding modes of the ligands

The **L** can be arranged in *anti-anti-anti* (AAA), *anti-anti-gauche* (AAG), *anti-gauche-anti* (AGA), *anti-gauche-gauche* (AGG), *gauche-anti-gauche* (GAG) and *gauche-gauche-gauche* (GGG) conformations, and based on the relative orientation of the C=O (or N-H) groups, each conformation adopts a *cis* or *trans* arrangement.¹³ The A and G conformations are given when the C-C-C-C torsion angle (θ) is $180 \geq \theta > 90^\circ$ and $0 \leq \theta \leq 90^\circ$, respectively. Due to the difference in the orientations of the pyridyl nitrogen atom positions, three more orientations, *anti-anti*, *syn-anti* and *syn-syn*, are possible for the **L**

ligand.^{13d} Based on this descriptor, the ligand conformations of complexes 1–8 are assigned and listed in Table 2. The various ligand conformations and dihedral angles between the two pyridyl ligands indicate that the **L** ligand is sufficiently flexible to adjust to the stereochemical requirements for the formation of the complexes 1–8, which adopts the conformation that maximize their intra- and intermolecular forces.

Various bonding modes are observed for the polycarboxylate ligands in 1–8. The 2,5-PDC²⁻ ligand in complex 1 chelates and bridges two metal centers through the nitrogen atom, an adjacent carboxylate oxygen and a remote carboxylate oxygen atom, Fig. 9(a). The 2,6-PDC²⁻ ligand in complex 2 coordinates to one metal center through the nitrogen atom and two oxygen atoms from the two carboxylate groups in a linear fashion, which also coordinates to another metal center through one oxygen atom, Fig. 9(b). The 3,4-PDC²⁻ ligand in complex 3 bridges two metal centers through the nitrogen atom and one of the oxygen atoms of the carboxylate group opposite to the nitrogen atom, Fig. 9(c). In a marked contrast to the coordination mode of Fig. 9(b), one oxygen atom of the 2,6-PDC²⁻ ligand in complex 4 bridges two metal centers, Fig. 9(d). The 1,3,5-HBTC²⁻ and 1,2,3-HBTC²⁻ ligands in complexes 5 and 6 bridge two metal centers through two oxygen atoms from two carboxylate groups, Fig. 9(e) and (f),

Table 2 The ligand conformations and the corresponding angles for 1–8

| Compounds | Diagram | Torsion angle (°) | Conformation | Dihedral angle (°) |
|-----------|---|-----------------------|-----------------------------|--------------------|
| 1 |  | -176.2, -180.0, 176.2 | AAA, <i>trans syn-syn</i> | 0 |
| 2 |  | 179.9, -180.0, -179.9 | AAA, <i>trans anti-anti</i> | 0 |
| 3 |  | -73.3, 180.0, 73.3 | GAG, <i>trans syn-syn</i> | 0 |
| 4 |  | 179.6, 176.2, 174.3 | AAA, <i>trans anti-anti</i> | 7.2 |
| 5 |  | -69.0, 180.0, 69.0 | GAG, <i>trans anti-anti</i> | 0 |
| 6 |  | 179.3, -180.0, -179.3 | AAA, <i>trans anti-anti</i> | 0 |
| |  | 170.0, 179.7, -175.3 | AAA, <i>trans anti-anti</i> | 23.0 |
| 7 |  | -170.0, -177.6, 172.1 | AAA, <i>trans anti-anti</i> | 2.3 |
| |  | 97.2, -36.6, 97.2 | AGA, <i>trans syn-syn</i> | 80.0 |
| 8 |  | -178.1, 73.2, 179.3 | AGA, <i>trans anti-anti</i> | 0 |

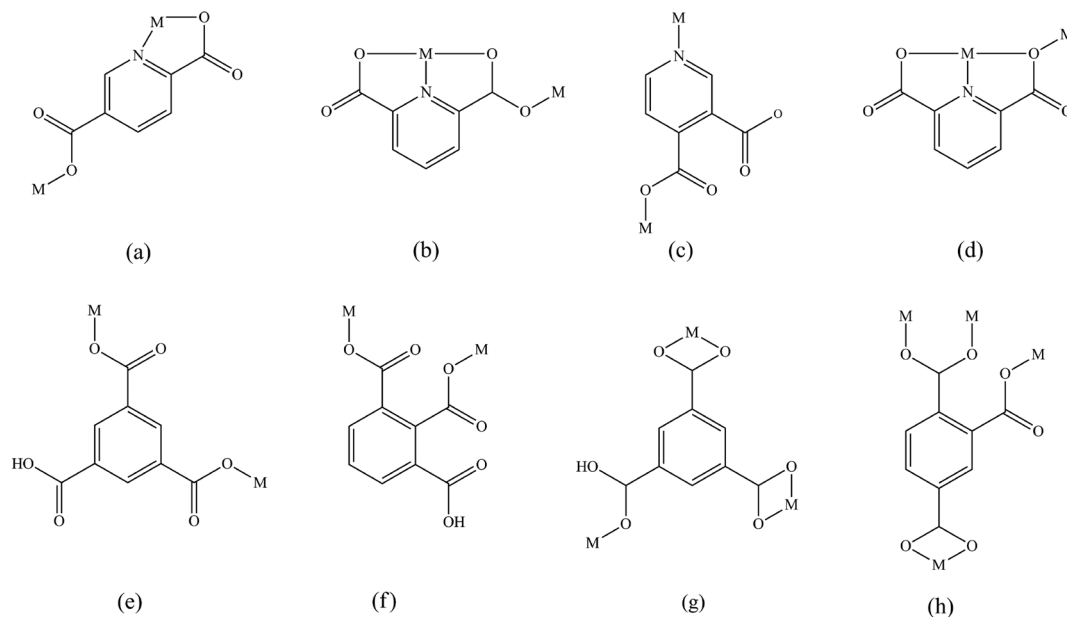


Fig. 9 The bonding modes found for the carboxylate ligands in 1–8.

whereas the 1,3,5-HBTC²⁻ ligand in complex 7 chelates and bridges three metal centers, Fig. 9(g). The 1,2,4-BTC³⁻ ligand in complex 8 adopts the $\mu_4\text{-}\eta^1, \eta^1, \eta^1, \eta^1$ mode, Fig. 9(h).

Thermal gravimetric analyses

Thermal gravimetric analyses (TGA) were carried out to examine the thermal stabilities of 1–8. The samples were heated in nitrogen gas at a pressure of 1 atm with a heating rate of 10 °C min⁻¹ and finished at 900 °C, Fig. S1† and S2† and Table 3. The TGA curve shows that 1 is stable up to 150 °C. A total weight loss of 9.2% occurred between 150 and 200 °C, presumably due to the removal of the cocrystallized H₂O (calcd 8.7%). The weight loss of 75.1% in 300–570 °C can be ascribed to the decomposition of the L and 2,5-PDC²⁻ ligands (calcd 75.6%). Complex 2 is stable up to 250 °C. The weight loss of 82.3% that occurred between 250 and 650 °C can be ascribed to the decomposition of the L and 2,6-PDC²⁻ ligands (calcd 82.8%). Complex 3 is stable up to 40 °C. A total weight loss of 19.6% occurred between 40 and 150 °C, presumably due to the removal of the cocrystallized H₂O (calcd 19.2%). The weight loss of 66.4% in 250–530 °C can be ascribed to the decomposition of the L and 3,4-PDC²⁻ ligands (calcd 66.9%).

Table 3 The thermal properties of 1–8

| Complex | Weight loss of H ₂ O, °C (found/calcd., %) | Weight loss of L and carboxylate, °C (found/calcd., %) |
|---------|---|--|
| 1 | 150–200 (9.2/8.7) | 300–570 (75.1/75.6) |
| 2 | 40–150 (19.6/19.2) | 250–650 (82.3/82.8) |
| 3 | 50–170 (13.8/13.5) | 260–530 (69.1/69.6) |
| 4 | 90–150 (5.0/5.5) | 340–580 (88.1/88.6) |
| 5 | 90–200 (7.5/7.1) | 230–570 (77.4/77.3) |
| 6 | 40–150 (13.2/13.7) | 300–620 (70.2/70.7) |
| 7 | | 350–510 (67.2/67.7) |
| 8 | | |

Complex 4 is stable up to 50 °C. A total weight loss of 13.8% occurred between 50 and 170 °C, presumably due to the removal of the cocrystallized H₂O (calcd 13.5%). The weight loss of 69.1% in 260–530 °C can be ascribed to the decomposition of the L and 2,6-PDC²⁻ ligands (calcd 69.6%). Complex 5 is stable up to 340 °C. The weight loss of 88.1% that occurred between 340 and 580 °C can be ascribed to the decomposition of the L and 1,3,5-HBTC²⁻ ligands (calcd 88.6%). Complex 6 is stable up to 90 °C. A total weight loss of 5.0% occurred between 90–150 °C, presumably due to the removal of the cocrystallized H₂O (calcd 5.5%). The weight loss of 77.4% in 230–570 °C can be ascribed to the decomposition of the L and 1,2,3-HBTC²⁻ ligands (calcd 77.3%). Complex 7 is stable up to 90 °C. A total weight loss of 7.5% occurred between 90 and 200 °C, presumably due to the removal of the cocrystallized H₂O (calcd 7.1%). The weight loss of 70.2% in 300–620 °C can be ascribed to the decomposition of the L and 1,3,5-HBTC²⁻ ligands (calcd 70.7%). Complex 8 is stable up to 40 °C. A total weight loss of 13.2% occurred between 40 and 150 °C, presumably due to the removal of the cocrystallized H₂O (calcd 13.7%). The weight loss of 67.2% in 210–500 °C can be ascribed to the decomposition of the L and 1,2,4-BTC³⁻ ligands (calcd 67.7%).

The results show that the complexes 1, 3, 4, 5–8 are stable up to 40–150 °C and the first weight losses that are due to the removal of cocrystallized and the bonded water molecules occurred in 40–200 °C. The TGA results also show that complexes 1–8 are thermally stable and the organic ligands decomposed at temperatures above 230 °C.

Luminescent properties

The emission spectra of the free organic ligands and complexes 1–8 were measured in the solid state at room temperature, Fig. S7† and Table 4. The dipyriddy amide ligand L and

Table 4 Luminescent properties of carboxylic acids and 1–8 in the solid state

| Compound | $\lambda_{\text{ex}}/\lambda_{\text{em}}$ (nm) | Compound | $\lambda_{\text{ex}}/\lambda_{\text{em}}$ (nm) |
|--------------------------|--|----------|--|
| L | 376/415 | 3 | 346/405 |
| 1,2,3-H ₃ BDC | 295/319 | 4 | 326/407 |
| 1,2,4-H ₃ BDC | 310/343 | 5 | 353/420 |
| 1,3,5-H ₃ BDC | 301/325 | 6 | 360/405 |
| 1 | 332/420 | 7 | 349/406 |
| 2 | 361/421 | 8 | 323/419 |

the carboxylic ligands 1,2,3-H₃BDC, 1,2,4-H₃BDC and 1,3,5-H₃BDC show emissions in the range of 319–415 nm, which may be tentatively ascribed to the intraligand (IL) $n \rightarrow \pi^*$ or $\pi \rightarrow \pi^*$ transitions, whereas 2,5-H₂PDC, 2,6-H₂PDC and 3,4-H₂PDC do not emit. The red and blue shifts with respect to the organic ligands observed for complexes 1–8 are most probably due to the different ligand conformations and coordination modes adopted by the organic ligands and the formation of different structural types. Since the Zn(II) and Cd(II) ions are hardly oxidized or reduced, it is not probable to assume that the emissions of 1–8 are due to a ligand-to-metal charge transfer (LMCT) or a metal-to-ligand charge transfer (MLCT). These emissions can most probably be attributed to an intraligand and/or ligand-to-ligand charge transfer (LLCT).²²

Conclusions

Eight new Zn(II) and Cd(II) coordination polymers have been synthesized under hydrothermal conditions, which show 1D, 2D and 3D structures. The structures of complexes 1–3, which contain Zn(II) ions and L ligands, are directed by the isomeric 2,5-, 2,6- and 3,4-PDC²⁻ ligands, resulting in 2D hcb layers with interdigitation and π - π stacking interactions for 1 and 2 and 1D ladders for 3, respectively. The isomeric effect of the HBTC²⁻ ligand is observed for 6 and 7, which resulted in a 3D coordination network with the dia topology and a double layer coordination network with the (6³)(6⁶)-3,4L88 topology, respectively. Structural comparisons between 2 and 4 and 5 and 7 reveal that the identity of the metal center is important in determining the structural diversity. A rare (6⁵·8)-hxc-d-4-P2/c topology is shown for 8. The structural types of 1–8 are a marked contrast to those reported for the Zn(II) and Cd(II) coordination polymers containing L and dicarboxylate ligands.^{10a} The results indicate that the benzenetricarboxylates are better auxiliary spacer ligands than pyridinedicarboxylates and benzenedicarboxylates^{10a} for the formation of di(pyridyl)adipoamide-based Zn(II) and Cd(II) coordination polymers with higher dimensionality. The conformations of the L ligands are subject to the changes of the polycarboxylate ligands and metal centers, resulting in different structural types found in 1–8.

Acknowledgements

We are grateful to the National Science Council of the Republic of China for support. DMP acknowledges the Ministry of Education and Science of Russia (grant 14.B25.31.0005). We

also thank Miss C.-W. Lu of the Instrumentation Center, National Taiwan University, for CHNS (EA) analysis experiments.

References

- (a) E. R. T. Tiekink and J. J. Vittal, *Frontiers in Crystal Engineering*, John Wiley & Sons, Ltd., England, 2006; (b) R. Robson, B. E. Abrahams, S. R. Batten, R. W. Gable, B. F. Hoskins and J. Lieu, *Supramolecular Architecture*, ACS publications, Washington, DC, 1992; (c) O. M. Yaghi, H. Li, C. Davis, D. Richardson and T. L. Groy, *Acc. Chem. Res.*, 1998, 31, 474; (d) C. B. Aakeröy and K. R. Seddon, *Chem. Soc. Rev.*, 1993, 22, 397; (e) M. Fujita and K. Ogura, *Coord. Chem. Rev.*, 1996, 148, 249; (f) C. B. Aakeröy, N. R. Champness and C. Janiak, *CrystEngComm*, 2010, 12, 22; (g) L. Carlucci, G. Ciani and D. M. Proserpio, *Coord. Chem. Rev.*, 2003, 246, 247; (h) M. O'Keeffe, M. A. Peskov, S. J. Ramsden and O. M. Yaghi, *Acc. Chem. Res.*, 2008, 41, 1782.
- (a) S. R. Batten and R. Robson, *Angew. Chem., Int. Ed.*, 1998, 37, 1460; (b) D. Braga and F. Grepioni, *Acc. Chem. Res.*, 2000, 33, 601; (c) S. Kitagawa, R. Kitaura and S. Noro, *Angew. Chem., Int. Ed.*, 2004, 43, 2334.
- (a) G. A. Jeffery, *An Introduction to Hydrogen Bonding*, Wiley, Chichester, 1997; (b) G. R. Desiraju and T. Steiner, *The Weak Hydrogen bond in Structural Chemistry and Biology*, Oxford University Press, Oxford, 1999; (c) A. M. Beatty, *CrystEngComm*, 2001, 51, 1.
- (a) H. Schmidbaur, *Chem. Soc. Rev.*, 1995, 24, 391; (b) P. Pyykkö, *Chem. Rev.*, 1997, 97, 597; (c) O. Navon, J. Bernstein and V. Khodorkovsky, *Angew. Chem., Int. Ed. Engl.*, 1997, 36, 601; (d) Q. Chu, Z. Wang, Q. Huang, C. Yan and S. Zhu, *J. Am. Chem. Soc.*, 2001, 123, 11069; (e) M. O. Sinnokrot and C. D. Sherrill, *J. Am. Chem. Soc.*, 2004, 126, 7690; (f) A. L. Pickering, D.-L. Long and L. Gronin, *Inorg. Chem.*, 2004, 43, 4953.
- (a) H.-H. Li, Z.-R. Chen, J.-Q. Li, C.-C. Huang, Y.-F. Zhang and G.-X. Jia, *Cryst. Growth Des.*, 2006, 6, 1813; (b) M. O. Awaleh, A. Badia and F. Brisse, *Cryst. Growth Des.*, 2006, 6, 2674; (c) Y.-H. Wang, K.-L. Chu, H.-C. Chen, C.-W. Yeh, Z.-K. Chan, M.-C. Suen and J.-D. Chen, *CrystEngComm*, 2006, 8, 84; (d) C.-Y. Lin, Z.-K. Chan, C.-W. Yeh, C.-J. Wu, J.-D. Chen and J.-C. Wang, *CrystEngComm*, 2006, 8, 841.
- X. H. Bu., W. Chen, W. F. Hou, R. H. Zhang and F. Brisse, *Inorg. Chem.*, 2002, 41, 3477.
- A. J. Blake, N. R. Champness, P. A. Cooke, J. E. B. Nicolson and C. J. Wilson, *J. Chem. Soc., Dalton Trans.*, 2000, 3811.
- S. R. Batten, N. R. Champness, X.-M. Chen, J. Garcia-Martinez, S. Kitagawa, L. Öhrström, M. O'Keeffe, M. P. Suh and J. Reedijk, *Pure Appl. Chem.*, 2013, 85, 1715.
- (a) M. Du, X.-J. Jiang and X.-J. Zhao, *Chem. Commun.*, 2005, 5521; (b) M. Du, Z.-H. Zhang, X.-G. Wang, L.-F. Tang and X.-J. Zhao, *CrystEngComm*, 2008, 10, 1855; (c) M. Du, X.-J. Jiang and X.-J. Zhao, *Inorg. Chem.*, 2007, 46, 3984; (d) J. Yang, J.-F. Ma, Y.-Y. Liu, J.-C. Ma and S. R. Batten, *Cryst.*

- Growth Des.*, 2009, 9, 1894; (e) X.-L. Wang, J. Luan, F.-F. Sui, H.-Y. Lin, G.-C. Liu and C. Xu, *Cryst. Growth Des.*, 2013, 13, 3561.
- 10 (a) P.-C. Cheng, P.-T. Kuo, Y.-H. Liao, M.-Y. Xie, W. Hsu and J.-D. Chen, *Cryst. Growth Des.*, 2013, 13, 623; (b) J.-J. Cheng, Y.-T. Chang, C.-J. Wu, Y.-F. Hsu, C.-H. Lin, D. M. Proserpio and J.-D. Chen, *CrystEngComm*, 2012, 14, 537; (c) M.-J. Sie, Y.-J. Chang, P.-W. Cheng, P.-T. Kuo, C.-W. Yeh, C.-F. Cheng, J.-D. Chen and J.-C. Wang, *CrystEngComm*, 2012, 14, 5505.
- 11 <http://rcsr.anu.edu.au/>.
- 12 M. O'Keeffe, M. A. Peskov, S. J. Ramsden and O. M. Yaghi, *Acc. Chem. Res.*, 2008, 41, 1782.
- 13 (a) Y.-F. Hsu, C.-H. Lin, J.-D. Chen and J.-C. Wang, *Cryst. Growth Des.*, 2008, 8, 1094; (b) Y.-F. Hsu, H.-L. Hu, C.-J. Wu, C.-W. Yeh, D. M. Proserpio and J.-D. Chen, *CrystEngComm*, 2009, 11, 168; (c) Y.-F. Hsu, W. Hsu, C.-J. Wu, P.-C. Cheng, C.-W. Yeh, W.-J. Chang, J.-D. Chen and J.-C. Wang, *CrystEngComm*, 2010, 12, 702; (d) P.-C. Cheng, C.-W. Yeh, W. Hsu, T.-R. Chen, H.-W. Wang, J.-D. Chen and J.-C. Wang, *Cryst. Growth Des.*, 2012, 12, 943.
- 14 (a) XSCANS, Release, 2.1, Siemens Energy & Automation, Inc, Madison, Wisconsin, USA, 1995; (b) Bruker AXS, APEX2, V2008.6; SAD ABS V2008/1; SAINT+ V7.60A; SHELXTL V6.14, Bruker AXS Inc., Madison, Wisconsin, USA, 2008.
- 15 G. M. Sheldrick, *Acta Crystallogr., Sect. A: Found. Crystallogr.*, 2008, 64, 112.
- 16 A. W. Addison, T. N. Rao, J. Reedijk, J. V. Rijn and G. C. Verschoor, *J. Chem. Soc., Dalton Trans.*, 1984, 1349.
- 17 V. A. Blatov, *Struct. Chem.*, 2012, p. 955, See also: <http://www.topos.samsu.ru/>.
- 18 T. G. Mitina and V. A. Blatov, *Cryst. Growth Des.*, 2013, 13, 1655.
- 19 V. A. Blatov, *Acta Crystallogr., Sect. A: Found. Crystallogr.*, 2007, 63, 329.
- 20 E. V. Alexandrov, V. A. Blatov, A. V. Kochetkov and D. M. Proserpio, *CrystEngComm*, 2011, 13, 3947.
- 21 X.-L. Wang, B. Mu, H.-Y. Lin, S. Yang, G.-C. Liu, A.-X. Tian and J.-W. Zhang, *Dalton Trans.*, 2012, 41, 11074, The net was erroneously described including 2-c nodes in the point symbol, thus preventing to recognize the uninodal nature of the $(6^5.8)\text{-hxg-d-}4\text{-}P2/c$ 4-c net.
- 22 (a) L.-F. Ma, L.-Y. Wang, J.-L. Hu, Y.-Y. Wang and G.-P. Yang, *Cryst. Growth Des.*, 2009, 9, 5334; (b) D. Sun, Z.-H. Yan, V. A. Blatov, L. Wang and D.-F. Sun, *Cryst. Growth Des.*, 2013, 13, 1277.